Part II
Plastic Analysis of Plates and Shells

Professor Tomasz Wierzbicki

Contents

1 Fundamentals

This part of the lecture notes is concerned with the development of the theory of small and moderately large deflections of plastic plates and shells. What differentiates the elastic and plastic theory of structures is the constitutive behavior. The other two groups of equations ie, the equations of equilibrium, Eq.(252 and 253 of Part I), and the strain-displacement relations remain the same. This chapter focuses on the development of constitutive equations for plates and shells. Three new concepts will be introduced:

- Plastic incompressibility
- Yield conditions
- Associated flow rule

Each of the above concepts will be briefly described.

1.1 Plastic Incompressibility

The explanation of this concept requires going back to the equation of the 3-D elasticity. Recall the relationship between the volumetric strain ε_{ii} and the hydrostatic pressure.

$$\varepsilon_{ii} = \frac{1}{K}p \tag{1}$$

where $p = \frac{1}{3}\sigma_{ii}$ is the mean stress and K is the bulk modulus defined by

$$K = \frac{E}{3(1 - 2\nu)} \tag{2}$$

The physical meaning of ε_{ii} is the relative change of volume

$$\varepsilon_{ii} = \varepsilon_{11} + \varepsilon_{22} + \varepsilon_{33} = \frac{dV}{V} \tag{3}$$

There is an overwhelming experimental evidence that plastic deformations do not produce any volume change of the material, $dV = 0$ even though the hydrostatic pressure is very high. This means that $\varepsilon_{ii} = 0$. Strictly speaking the plastic part of the strain tensor will vanish, $\varepsilon_{ii}^p = 0$. In view of Eq.(1) the bulk modulus should go to infinity, which happens when $\nu = 0.5$. Thus for a plastic incompressible material the Poisson ratio should be equal to one half. In the theory of plates and shells the material incompressibility is equivalent to

$$\varepsilon_{\alpha\alpha} = -\varepsilon_{33} \tag{4}$$

Therefore, a joint action of any in-plane direct strains produces strain in the thickness direction ε_{33}. There are no constraints for the thickness h to become thinner or thicker. The incompressibility condition will thus be automatically satisfied for thin-walled structures. The only inconsistency is that in the constitutive equations for plates and shells, the thickness is considered to be constant while in reality there will be a small change, according to Eq.(4).

1.2 Yield Condition

The starting point of the analysis is the Hooke's law for plane stress

$$\sigma_{\alpha\beta} = \frac{E}{1 - \nu^2}\left[(1 - \nu)\varepsilon_{\alpha\beta} + \nu\epsilon_{\gamma\gamma}\delta_{\alpha\beta}\right] \tag{5}$$

introduced earlier, see Eq.(34 of Part I). The inverted form of the above equation is

$$\varepsilon_{\alpha\beta} = \frac{1 - \nu}{E}\left[\sigma_{\alpha\beta} - \frac{\nu}{1 + \nu}\sigma_{\gamma\gamma}\delta_{\alpha\beta}\right] \tag{6}$$

Huber postulated in 1904 that yielding of the material occurs when the elastic (distortional) energy in a unit volume reaches a critical value. The strain energy density is defined

$$\frac{1}{2}\sigma_{\alpha\beta} \cdot \varepsilon_{\alpha\beta} = C \tag{7}$$

Using Eq.(6) and the incompressibility $\nu = \frac{1}{2}$, the strain energy can be expressed in terms of the plane stress tensor as

$$\frac{1+\nu}{2E}\left[\sigma_{\alpha\beta}\sigma_{\alpha\beta} - \frac{1}{3}\sigma_{\alpha\alpha}\sigma_{\beta\beta}\right] = C \tag{8}$$

or

$$3\sigma_{\alpha\beta}\sigma_{\alpha\beta} - \sigma_{\alpha\alpha}\sigma_{\beta\beta} = \frac{2EC}{1+\nu} = \mathbf{C_1} \tag{9}$$

The unknown calibration constant $\mathbf{C_1}$ can be determined from uniaxial tension or shear test. Consider uniaxial tension

$$\sigma_{\alpha\beta} = \begin{vmatrix} \sigma_{11} & 0 \\ 0 & 0 \end{vmatrix} \tag{10}$$

Expanding the expression on the left hand side of Eq.(9), one gets

$$3\sigma_{11}^2 - \sigma_{11}^2 = 2\sigma_{11}^2 = \mathbf{C_1} \tag{11}$$

Yielding occurs when $\sigma_{11} = \sigma_y$, where σ_y is the uniaxial yield stress of the material. Thus $\mathbf{C_1} = 2\sigma_y^2$ and the final form of the plane stress yield condition reads

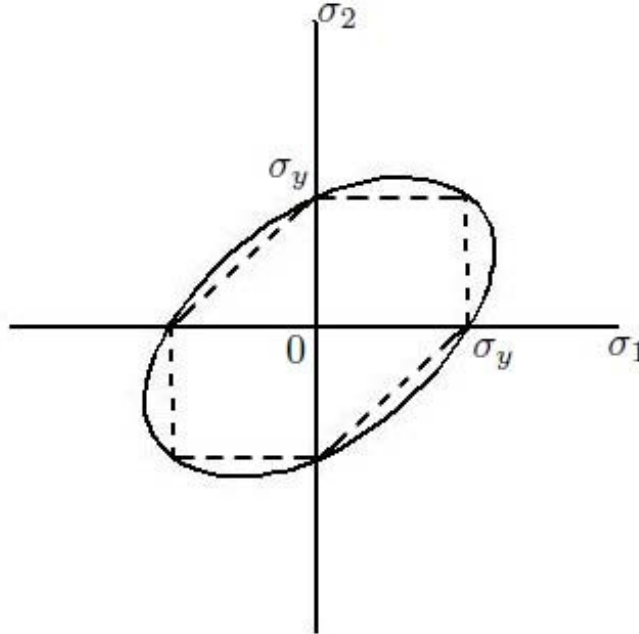$$3\sigma_{\alpha\beta}\sigma_{\alpha\beta} - \sigma_{\alpha\alpha}\sigma_{\beta\beta} = 2\sigma_y^2 \tag{12}$$

In the expanded notation, Eq.(12) takes the following form

$$\sigma_{11}^2 - \sigma_{11}\sigma_{22} + \sigma_{22}^2 + 3\sigma_{12}^2 = \sigma_y^2 \tag{13}$$

In the principal stress coordinate system $\sigma_{12} = 0$, and Eq.(13) reduces to

$$\sigma_1^2 - \sigma_1\sigma_2 + \sigma_2^2 = \sigma_y^2 \tag{14}$$

A graphical representation of Eq.(14) is the Huber-Mises ellipse (full line). The broken line in the same figure

represents the Tresca yield condition which is derived from an entire different hypothesis. Tresca assumed that yielding of the material occurs when the maximum shear stress reaches a critical value. The maximum shear stress can be easily expressed in terms of principal stresses

$$\tau_{max} = max\left\{\frac{|\sigma_1 - \sigma_2|}{2}, \frac{|\sigma_2 - \sigma_3|}{2}, \frac{|\sigma_3 - \sigma_1|}{2}\right\} \tag{15}$$

In the case of plane stress $\sigma_3 = 0$ and Eq.(15) reduce to

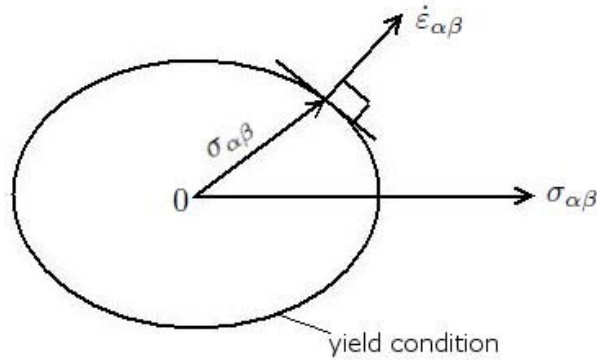$$max\left\{|\sigma_1 - \sigma_2|, |\sigma_2|, |\sigma_1|\right\} = 2k = \sigma_y \tag{16}$$

where k is the yield stress in shear. A graphical representation of Eq.(16) is the Tresca Hexagon.

1.3   Associated Flow Rule

Let us define the yield function F by

$$F \equiv 3\sigma_{\alpha\beta}\sigma_{\alpha\beta} - \sigma_{\alpha\alpha}\sigma_{\beta\beta} - 2\sigma_y \tag{17}$$

It was observed experimentally that increments or rates of the plastic strain tensor $\dot{\varepsilon}_{\alpha\beta}$ are normal to the yield condition

Mathematically, the normality condition is expressed as

$$\dot{\varepsilon}_{\alpha\beta} = \dot{\lambda}\frac{\delta F(\sigma_{\alpha\beta})}{\delta\sigma_{\alpha\beta}} \tag{18}$$

Performing the differentiation one finally gets the flow rule for plane stress.

$$\dot{\varepsilon}_{\alpha\beta} = 2\dot{\lambda}(3\sigma_{\alpha\beta} - \sigma_{\alpha\alpha}\delta_{\alpha\beta}) \tag{19}$$

where $\dot{\lambda}$ is the proportionality constant.

It is possible to invert the flow rule with the help of the yield condition. The proportionality constant can be eliminated between Eq.(12) and (19) and the stresses can be uniquely expressed in terms of components of the strain rates by

$$\sigma_{\alpha\beta} = \sqrt{\frac{2}{3}}\sigma_y\frac{\dot{\varepsilon}_{\alpha\beta} + \dot{\varepsilon}_{\alpha\alpha}\delta_{\alpha\beta}}{\sqrt{\dot{\varepsilon}_{\alpha\beta}\dot{\varepsilon}_{\alpha\beta} + \dot{\varepsilon}_{\alpha\alpha}\dot{\varepsilon}_{\beta\beta}}} \tag{20}$$

In the principal coordinate system

$$\sigma_{\alpha\beta} = \left|\begin{array}{cc} \sigma_1, & 0 \\ 0, & \sigma_2 \end{array}\right|, \quad \varepsilon_{\alpha\beta} = \left|\begin{array}{cc} \varepsilon_1, & 0 \\ 0, & \varepsilon_2 \end{array}\right| \tag{21}$$
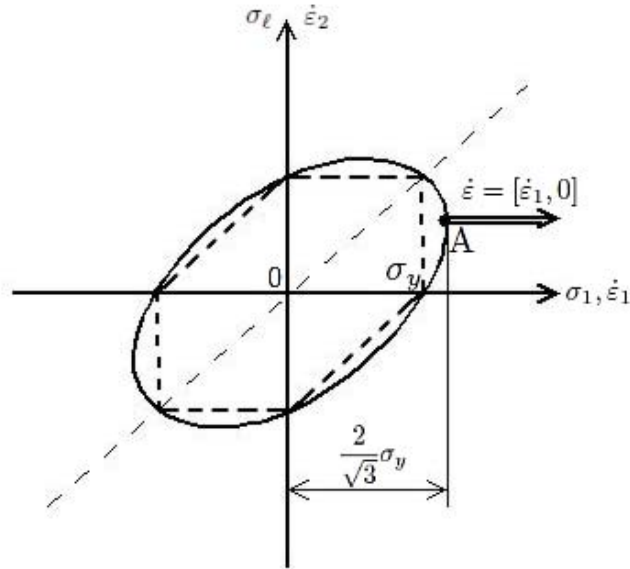
4

and Eq.(20) reduces to

$$
\left.
\begin{aligned}
\sigma_1 &= \frac{\sigma_y}{\sqrt{3}} \frac{2\dot\varepsilon_1 + \dot\varepsilon_2}{\sqrt{\dot\varepsilon_1^2 + \dot\varepsilon_1\dot\varepsilon_2 + \dot\varepsilon_2^2}} \\[2mm]
\sigma_2 &= \frac{\sigma_y}{\sqrt{3}} \frac{2\dot\varepsilon_2 + \dot\varepsilon_1}{\sqrt{\dot\varepsilon_1^2 + \dot\varepsilon_1\dot\varepsilon_2 + \dot\varepsilon_2^2}}
\end{aligned}
\right\}
\tag{22}
$$

Finally, from Eq.(20) one can easily calculate the so-called plastic dissipation rate $\dot D$.

$$
\dot D = \sigma_{\alpha\beta}\dot\varepsilon_{\alpha\beta} = \sqrt{\frac{2}{3}}\sigma_y\sqrt{\dot\varepsilon_{\alpha\beta}\dot\varepsilon_{\alpha\beta} + \dot\varepsilon_{\alpha\alpha}\dot\varepsilon_{\beta\beta}}
\tag{23}
$$

In particular, the state $\varepsilon_{22} = \varepsilon_{12} = 0$ corresponds to the transverse plane strain in which the dissipation rate reduces to

$$
\dot D = \left(\frac{2}{\sqrt{3}}\sigma_y\right)\dot\varepsilon_{11}
\tag{24}
$$

This state is represented in the figure by point A where the stress coordinates are

$$
\sigma_1 = \frac{2}{\sqrt{3}}\sigma_y
$$

$$
\sigma_2 = \frac{1}{\sqrt{3}}\sigma_y
\tag{25}
$$

Thus under the constraint $\dot\varepsilon_2 = 0$, there is a reaction stress $\sigma_2 = \frac{1}{2}\sigma_1$

2 Yield Conditions in the Space of Generalized Stresses

In the theory of the elastic structures the relationship between the generalized stresses and strain is obtained relatively easily. The Hooke's law is linear. Thus, integration of stresses through the thickness is straightforward where the Love-Kirchoff hypothesis is used. By contrast, in the case of plastic structures, the stress-strain rate relation are nonlinear and with the exception of few simple cases, the integration can not be performed.

Simple and surprisingly accurate results are obtained by replacing the solid cross-section by a sandwich section. The face plates of the thickness t each transmit in-plane stresses $\sigma_{\alpha\beta}$. The sandwich core of the thickness h transmits in-plane shear stresses.
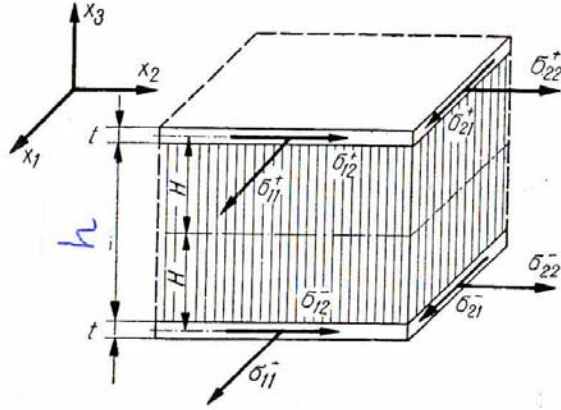
It is assumed that $h \gg t$ so that the distribution of stresses $\sigma_{\alpha\beta}$ over the thickness of the face plate is constant. The one-dimensional case of stress distribution is shown in the figure below.
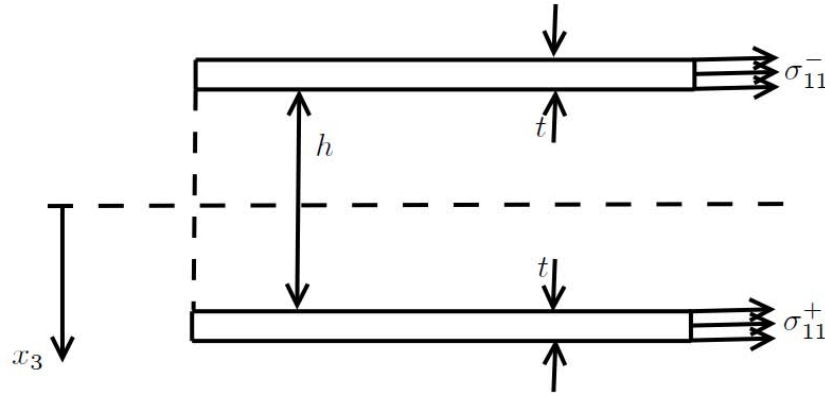
Thus, the stress resultant $N_{\alpha\beta}$ and stress couples $M_{\alpha\beta}$ are

$$N_{\alpha\beta} = (\sigma_{\alpha\beta}^{+} + \sigma_{\alpha\beta}^{-})t \tag{26}$$

$$M_{\alpha\beta} = (\sigma_{\alpha\beta}^{-} - \sigma_{\alpha\beta}^{+})t\frac{h}{2} \tag{27}$$

Consider a uniaxial case. If both the face plates are at yield $\sigma_{11}^{+} = \sigma_{11}^{-} = \sigma_y$. then from Eq.(26) the reference membrane force is

$$N_0 = 2\sigma_y t \tag{28}$$

while $M = 0$. In the case of pure bending $\sigma_{11}^{-} = \sigma_y, \sigma_{11}^{+} = -\sigma_y$ and the reference bending moment is

$$M_0 = \sigma_y t h \tag{29}$$

while the membrane force is zero. It is convenient to normalize the components of the membrane force and bending moment according to

$$n_{\alpha\beta} = \frac{N_{\alpha\beta}}{N_0}, \quad m_{\alpha\beta} = \frac{M_{\alpha\beta}}{M_0} \tag{30}$$

6

Then, the system of Eqs.(26) and (27) is equivalent to

$$\sigma_{\alpha\beta}^{+} = \sigma_y(n_{\alpha\beta} - m_{\alpha\beta}),$$

$$\sigma_{\alpha\beta}^{-} = \sigma_y(n_{\alpha\beta} + m_{\alpha\beta}) \tag{31}$$

Assuming that both upper and lower face plates of the sandwich structures are at yield, Eq.(31) can be inserted to the plane stress yield conditions given by Eq.(12). This leads to the following simultaneous system of equations

$$3n_{\alpha\beta}n_{\alpha\beta} - n_{\alpha\alpha}n_{\beta\beta} + 3m_{\alpha\beta}m_{\alpha\beta} - m_{\alpha\alpha}m_{\beta\beta} = 2 \tag{32}$$

$$3m_{\alpha\beta}n_{\alpha\beta} - m_{\alpha\alpha}n_{\beta\beta} = 0 \tag{33}$$

In particular, in the principal coordinate system Eqs.(32) and (33) reduce to

$$n_1^2 - n_1 n_2 + n_2^2 + m_1^2 - m_1 m_2 + m_2^2 = 1 \tag{34}$$

$$2n_1 m_1 + 2n_2 m_2 - n_1 m_2 - n_2 m_1 = 0 \tag{35}$$

Eqs.(32) and (35) can be represented as a surface $F(m_{\alpha\beta}, n_{\alpha\beta}) = 0$ in the six-dimensional space. Many special cases can be derived from Eqs.(32) and (33).

2.1 Pure Bending Action, $N_{\alpha\beta} = 0$ or $n_{\alpha\beta} = 0$

Equation(33) is identically satisfied and Eq.(32) yields

$$3m_{\alpha\beta}m_{\alpha\beta} - m_{\alpha\alpha}m_{\beta\beta} = 2 \tag{36}$$

or in physical quantities (see the normalization Eqs.(29) and (30))

$$3M_{\alpha\beta}M_{\alpha\beta} - M_{\alpha\alpha}M_{\beta\beta} = 2M_0^2 \tag{37}$$

In principal direction

$$M_1^2 - M_1 M_2 + M_2^2 = M_0^2 \tag{38}$$

It is interesting to note that Eq.(36) is exact, i.e. the same expression is obtained for solid and sandwich sections. Therefore, the six-dimensional yield surface given by Eqs.(32) and (33) is sufficiently accurate for practical applications. Note a formal analogy between the yield condition in plane stress, Eq.(17) and corresponding yield loci for moments, Eq.(36). Therefore, the expression for the flow rule and dissipation function can be readily written without derivation.

$$M_{\alpha\beta} = \sqrt{\frac{2}{3}} M_0 \frac{\dot{\kappa}_{\alpha\beta} + \dot{\kappa}_{\gamma\gamma}\delta_{\alpha\beta}}{\sqrt{\dot{\kappa}_{\alpha\beta}\dot{\kappa}_{\alpha\beta} + \dot{\kappa}_{\alpha\alpha}\dot{\kappa}_{\beta\beta}}} \tag{39}$$

$$\dot{D}_b = M_{\alpha\beta}\dot{\kappa}_{\alpha\beta} = \sqrt{\frac{2}{3}} M_0 \sqrt{\dot{\kappa}_{\alpha\beta}\dot{\kappa}_{\alpha\beta} + \dot{\kappa}_{\alpha\alpha}\dot{\kappa}_{\beta\beta}} \tag{40}$$

2.2 Pure Membrane Action, $M_{\alpha\beta} = 0$ or $m_{\alpha\beta} = 0$

Eq.(33) is identically satisfied while Eq.(32) reduces to:

$$3n_{\alpha\beta}n_{\alpha\beta} - n_{\alpha\alpha}n_{\beta\beta} = 2 \tag{41}$$

In physical quantities the above equation reads

$$3N_{\alpha\beta}N_{\alpha\beta} - N_{\alpha\alpha}N_{\beta\beta} = 2N_0^2 \tag{42}$$

In principal directions

$$N_1^2 - N_1 N_2 + N_2^2 = N_0^2 \tag{43}$$

Both yield loci are represented by a Huber-Mises ellipse.

$$N_{\alpha\beta} = \sqrt{\frac{2}{3}} N_0 \frac{\dot{\varepsilon}_{\alpha\beta} + \dot{\varepsilon}_{\gamma\gamma}\delta_{\alpha\beta}}{\sqrt{\dot{\varepsilon}_{\alpha\beta}\dot{\varepsilon}_{\alpha\beta} + \dot{\varepsilon}_{\alpha\alpha}\dot{\varepsilon}_{\beta\beta}}} \tag{44}$$

$$\dot{D}_m = N_{\alpha\beta}\dot{\varepsilon}_{\alpha\beta} = \sqrt{\frac{2}{3}} N_0 \sqrt{\dot{\varepsilon}_{\alpha\beta}\dot{\varepsilon}_{\alpha\beta} + \dot{\varepsilon}_{\alpha\alpha}\dot{\varepsilon}_{\beta\beta}} \tag{45}$$

2.3 Cylindrical Shell

In a more general case in which both bending moments and membrane forces are developed, the four dimensional yield function $F(m_{\alpha\beta}, n_{\alpha\beta})$ can be defined by combining Eqs.(32) and (33). Then, the associated flow rule will define the direction of the generalized strain rates.
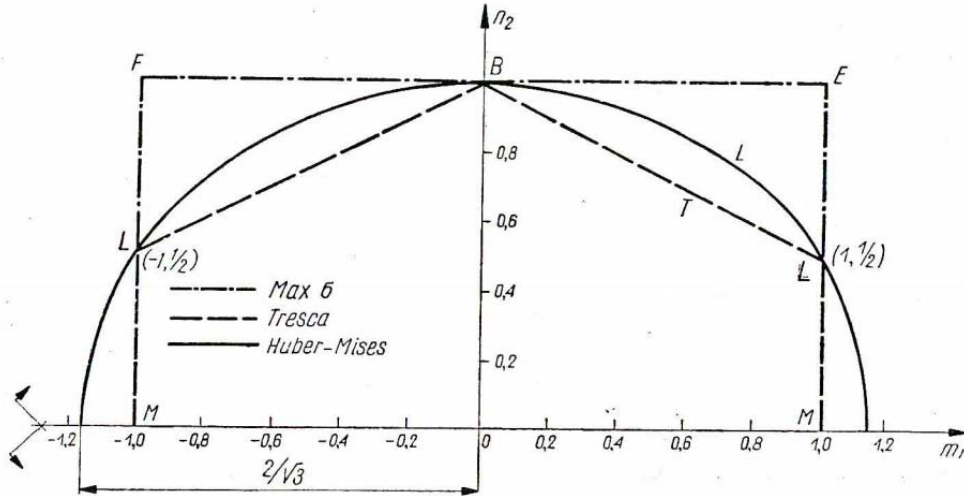
$$\dot{\kappa}_{\alpha\beta} = \dot{\lambda}\frac{\delta F}{\delta m_{\alpha\beta}}, \quad \dot{\varepsilon}_{\alpha\beta} = \dot{\lambda}\frac{\delta F}{\delta n_{\alpha\beta}} \tag{46}$$

For example, for a cylindrical shell with zero axial membrane force n_1

$$n_2^2 + \frac{3}{4}m_1^2 = 1, \quad m_2 = \frac{1}{2}m_1 \tag{47}$$

Combining Eqs.(46) and (47), the inverted constitutive equations are

$$n_2 = \frac{\dot{\varepsilon}_2}{\sqrt{\dot{\varepsilon}_2^2 + \frac{4}{3}\dot{\kappa}_1^2}}, \quad m_1 = \frac{\frac{4}{3}\dot{\kappa}_1^2}{\sqrt{\dot{\varepsilon}_2^2 + \frac{4}{3}\dot{\kappa}_1^2}} \tag{48}$$

The elliptical yield locus given by Eq.(47) is compared with the yield conditions corresponding to the Tresca and maximum stress yield criterion.

3 Principle of Virtual Velocity and Limit Analysis

In the theory of plasticity the incremental and rate formulations are equivalent. From the chain rule of differentiation

$$\delta\varepsilon_{\alpha\beta} = \frac{\delta\varepsilon_{\alpha\beta}}{\delta t}\delta t = \dot{\varepsilon}_{\alpha\beta}\delta t \tag{49}$$

The constitutive equation of plasticity, Eq.(20) is the homogenous equation of degree zero i.e.

$$\sigma_{\alpha\beta}(\dot{\varepsilon}_{\alpha\beta}) = \sigma_{\alpha\beta}(\frac{\delta\varepsilon_{\alpha\beta}}{\delta t}) = \sigma_{\alpha\beta}(\delta\varepsilon_{\alpha\beta}) \tag{50}$$

8

This property proves the equivalence of the global equilibrium equation expressed by $\delta\pi = 0$, Eq.(118 of Part I) and the principle of virtual velocity

$$\int_S (\dot{M}_{\alpha\beta}\dot{\kappa}_{\alpha\beta} + N_{\alpha\beta}\dot{\varepsilon}_{\alpha\beta})dS = \int_S p\dot{w}dS + \oint_\Gamma (N_{nn}\dot{u}_n + N_{nt}\dot{u}_t) \tag{51}$$

where (n, t) denotes the normal and tangential direction on the outer boundary Γ. It should be mentioned that Eq.(51) represents the condition of global equilibrium from which the local equilibrium equation can be derived. This has been done in Part I notes on the example of small (Eq. 101) and moderately large deflections of plates (Eq. 136). In the case of the bending theory of plates subjected to a transverse pressure loading, Eq.(51) reduces to

$$\int_S M_{\alpha\beta}\dot{\kappa}_{\alpha\beta}dS = \int_S p\dot{w}dS, \tag{52}$$

where S is the lateral surface of the shell. Note that for the principle of virtual velocity the static quantities $(M_{\alpha\beta}, p)$ must be in equilibrium. Similarly, the rate of generalized strains $\dot{\kappa}_{\alpha\beta}$ must be compatible with the displacement rate, $\dot{w}$. In Eq.(52) nothing is said about the relation between $M_{\alpha\beta}$ and $\dot{\kappa}_{\alpha\beta}$, so it is valid for any type of material.

3.1 Lower Bound Theorem

The limit analysis theorem for elastic-perfectly plastic structures provides bounds on the magnitude of external loads causing structural collapse. In this connection, two new concepts are introduced.

Any stress state $M_{\alpha\beta}^\circ$, p° satisfying:

- Equation of equilibrium (Eq. 101 of Part I)

- Stress (moments) boundary conditions (Eq. 102 of Part I)

- And not violating the yield condition, $F \le 0$

is called the *statically admissible state*. It can be proved that p° provides a lower bound for the exact limit load, $p^\circ \le p$. Example will follow.

3.2 Upper Bound Theorem

The main new concept is the *kinematically admissible velocity field* $\dot{w}^*$. This field represents the incipient collapse mode of a structure. It has to satisfy the kinematic boundary conditions (zero velocity or slopes) and should lead to unique expressions for the generalized strain rates $\dot{\kappa}_{\alpha\beta}^*$ from which the rate of plastic dissipation can be calculated, using Eq.(40). The corresponding collapse load $p*$ is defined by

$$\int_S M_{\alpha\beta}^* \dot{\kappa}_{\alpha\beta}^* dS \equiv \int_S p^* \dot{w}^* dS \tag{53}$$

It should be noted that $(\dot{\kappa}_{\alpha\beta}^*, \dot{w}^*)$ is a kinematically admissible state. At the same time, $(M_{\alpha\beta}^*, p^*)$ are generally not in equilibrium.

In order to prove the upper bound theorem consider a modified version of the principle of virtual work, Eq.(52):

$$\int_S M_{\alpha\beta}\dot{\kappa}_{\alpha\beta}^* dS = \int_S p\dot{w}^* dS \tag{54}$$

Equation (54) differs from Eq. (53) in that the starred quantities are replaced by exact values $(M_{\alpha\beta}, p)$ which are in equilibrium.

Subtracting side by side Eq.(54) from Eq.(53) one gets

$$\int_S (M_{\alpha\beta}^* - M_{\alpha\beta})\dot{\kappa}_{\alpha\beta}^* dS = \int_S (p^* - p)\dot{w}^* dS \tag{55}$$

According to Drucker's stability postulate the integrand $(M_{\alpha\beta}^* - M_{\alpha\beta})\dot{\kappa}_{\alpha\beta}^* \ge 0$ is non-negative for the convex yield condition and the associated flow rule. It follows then from Eq. (55) that $p^* \ge p$ provided that $\int_S \dot{w}^* dS > 0$. We have shown that the load intensity p^*, defined by Eq. (53), is always an upper bound on the actual collapse load p.

4 Applications

4.1 Bending of a Simply Supported Plate

Let us consider a simply supported circular plate subjected to the uniformly distributed transverse pressure p.
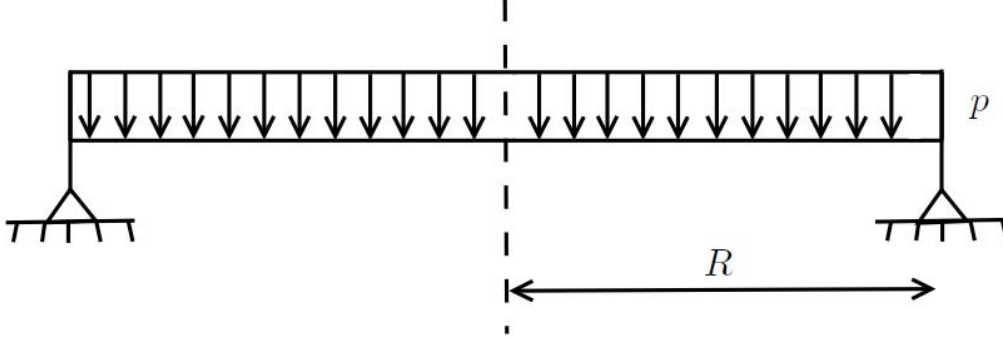
The internal stress state is defined by the radial and circumferential bending moments (M_r, M_θ). In view of the rotational symmetry the twisting moment vanishes. Therefore, the bending moments are principal bending moments $M_r = M_1$, $M_\theta = M_2$ and the yield condition Eq.(38) applies. The lower bound on the collapse load is calculated first.

Let us consider the hexagon inscribed into the von Mises ellipse. Boundary conditions

$$M_r = M_\theta \quad \text{at} \quad r = 0$$

$$M_r = 0 \quad \text{at} \quad r = R \tag{56}$$

dictate that the stress profile lies in the first quadrant, so that

$$0 < M_r^\circ < M_0$$

$$M_\theta = M_0 \tag{57}$$

The problem has been reduced to finding a distribution of the radial bending moment $M_r^\circ(r)$ satisfying the stress boundary condition and the equations of equilibrium. The equations of equilibrium of the circular plate, transferred from the rectangular coordinate system (Eq. 101 of Part I) to the polar coordinate system are

Force equilibrium

$$\frac{d}{dr}(rQ_r) + rp = 0 \tag{58}$$

Moment equilibrium

$$\frac{d}{dr}(rM_r) - M_\theta - rQ_r = 0 \tag{59}$$

where Q_r is the transverse shear force. Substituting $M_\theta = 0$ and eliminating Q_r between the above equations yields

$$\frac{d^2}{dr^2}(rM_r) = -pr \tag{60}$$

The solution of this equation satisfying the static (moment) boundary conditions, Eq.(56), is

$$M_r(r) = \frac{p}{6}(R^2 - r^2) \tag{61}$$

In particular, for $r = 0$, $M_r = M_\theta = M_0$ so that

$$p^\circ = \frac{6M_0}{R^2} \tag{62}$$

This expression provides a lower bound on the collapse load of the plate obeying the von Mises yield condition. Note that in deriving the above lower bound, nothing was said about the curvature rates $(\dot{\kappa}_r, \dot{\kappa}_\theta)$ or the strain rate field $\dot{w}$.

In order to derive an upper bound on the collapse load, one has to define the kinematic boundary conditions. For a simply supported plate the slope at the center should vanish and the velocity at the outer boundary is zero:

$$\frac{d\dot{w}}{dr} = 0 \quad \text{at} \quad r = 0 \tag{63}$$

$$\dot{w} = 0 \quad \text{at} \quad r = R \tag{64}$$

A specific form of Eq.(56) for a circular plate from which the upper bound load is calculated reads

$$2\pi \int_0^R \frac{2}{\sqrt{3}} M_0 \sqrt{(\dot{\kappa}_r^*)^2 + \dot{\kappa}_r^* \dot{\kappa}_\theta^* + (\dot{\kappa}_\theta^*)^2} \, r \, dr = 2\pi \int_0^R p^* \dot{w}^*(r) r \, dr \tag{65}$$

The left hand side represents the rate of plastic energy dissipation in the bending action integrated over the plate area, according to Eq.(40). The right hand side is the rate of work of external loading. The principal curvature are the radial and circumferential curvatures, defined by:

$$\dot{\kappa}_r = -\frac{d^2 w}{dr^2}, \quad \dot{\kappa}_\theta = \frac{-1}{r} \frac{d\dot{w}}{dr} \tag{66}$$

Let us assume a family of kinematically admissible velocity fields in the form

$$\dot{w}^*(r) = \dot{w}_0 [1 - (\frac{r}{R})^n] \tag{67}$$

where $\dot{w}_0$ is the central amplitude and n is a free parameter, to be determined. The above solutions satisfy identically the kinematic boundary conditions. Calculating the curvature rates, substituting to Eq.(65) and integrating gives the following expression for the load-carrying capacity:

$$p^* = \frac{M_0}{R^2} \frac{4}{\sqrt{3}} (1 + \frac{2}{n}) \sqrt{n^2 - n + 1} \tag{68}$$

The exponent n can now be chosen to minimize the magnitude of p^*. From the condition $\frac{dp^*}{dn} = 0$, one obtains the cubic algebraic equation

$$2n^3 - n^2 + 2n - 4 = 0 \tag{69}$$

whose real solution is $n = 1.15$. Substituting the optimum value of n into Eq.(61) the minimum value of the collapse load is

$$p^* = 6.85 \frac{M_0}{R^2} \tag{70}$$

The coefficient in the exact solution of this problem is 6.51 giving the error of some 14%. The reason for the error is that the present approximate solution does not satisfy the "static" boundary conditions, given by Eq. (56), and the local equation of equilibrium. Instead, the components of the bending moment are constant over the plate because the curvature rate ratio is fixed

$$\alpha = \frac{\dot{\kappa}_\theta}{\dot{\kappa}_r} = \frac{1}{n-1} \tag{71}$$
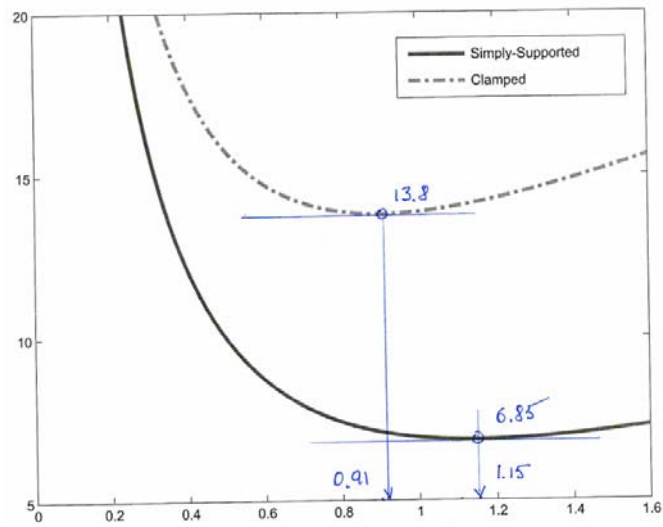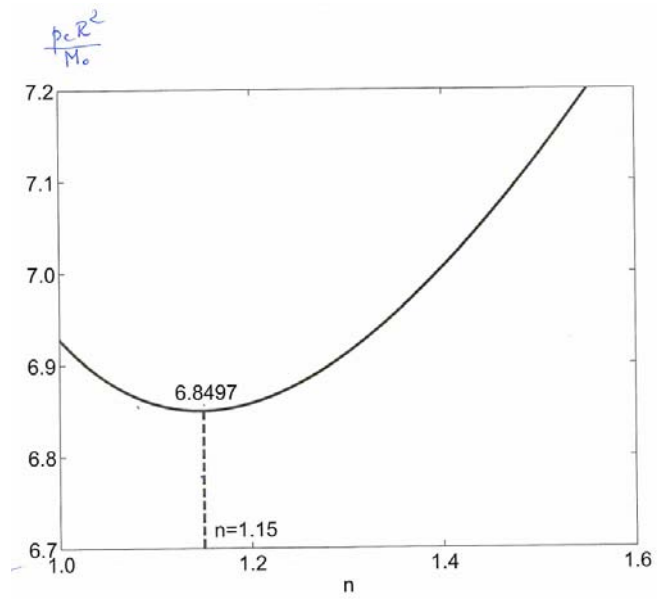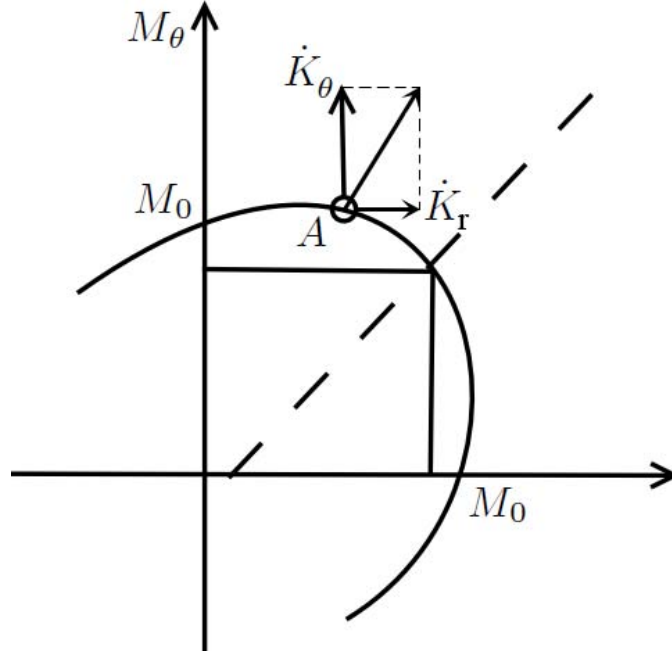
For $n = 1$, the vector of the curvature rate is normal to the M_r axis and the coordinates of the moment vector are

$$M_r = \frac{1}{\sqrt{3}}M_0 = 0.57M_0$$

$$(72)$$

$$M_\theta = \frac{2}{\sqrt{3}}M_0 = 1.15M_0$$

In the present case with $n = 1.15$ the magnitude of the bending moments are slightly different but constant, see point A in the figure above.

$$M_r = 0.69M_0$$

$$(73)$$

$$M_\theta = 1.14M_0$$

It is seen that the constant moment solution can satisfy neither plate equilibrium, Eq.(59), nor the stress boundary conditions. An important conclusion is that bounds in the collapse load $6 < p^* < 6.85$ were established through relatively simple calculations.

4.2   Concept of a Plastic Hinge, and Example of a Clamped Plate
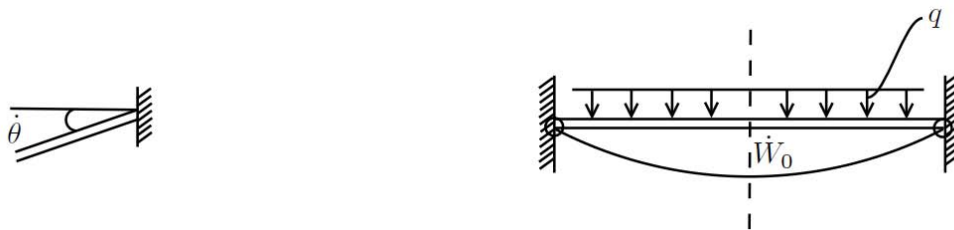
In order to extend the solution for the simply supported plate to the case of a clamped plate, a concept of the plastic hinge line should be introduced.

13

Elastic

hinge line

rigid - plastic

θ
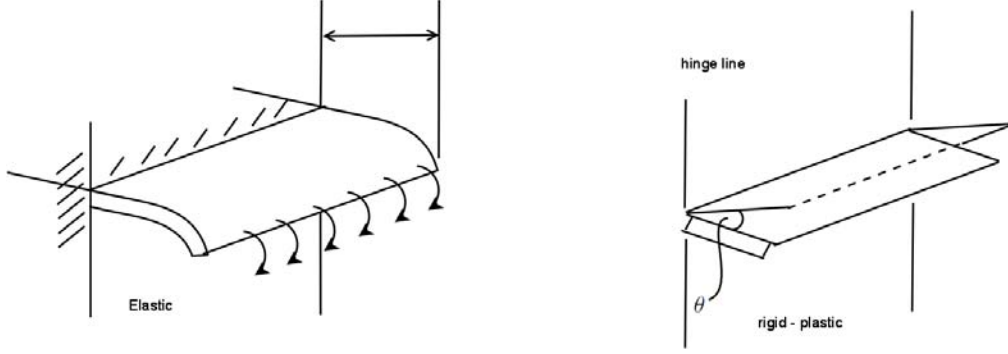
Clamped boundary conditions for an elastic plate require vanishing of the slope. Not so in the theory of plasticity. Consider the transverse plane strain loading (cylindrical bending) of a strip made of rigid-plastic material.

Δx

fully plastic bending moment $\dfrac{2M_0}{\sqrt{3}}$
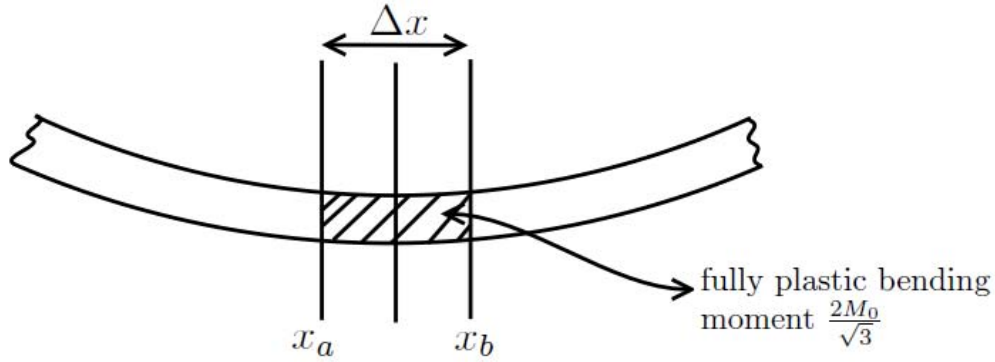
x_a x_b

Calculate the rate of plastic work over a small segment Δx

$$\dot{D} = \int_{x_a}^{x_b} M\dot{\kappa}\,dx = \int_{x_a}^{x_b} M\,d\dot{\theta} \tag{74}$$

where $\dot{\kappa}dx = d\dot{\theta}$ comes from the definition of a curvature as a change of the slope θ,

$$\dot{\kappa} = \frac{d\dot{\theta}}{dx} \tag{75}$$

For $\Delta x = x_b - x_a$ sufficiently small, the moment can be assumed to be constant and Eq.(65) is replaced by

$$\dot{D} = M_0 \int_{x_a}^{x_b} d\dot{\theta} = M_0\dot{\theta}\Big|_{x_a}^{x_b} = M_0\left[\dot{\theta}(x_b) - \dot{\theta}(x_a)\right] = M_0\Delta\dot{\theta} \tag{76}$$

where $\Delta\dot{\theta}$ is the relative rotation on both sides of the hinge.

In plastic plates and shells discontinuities in the rate of rotation $\Delta\dot{\theta}$ are admissible and should be included in the formulation. Referring to the case of the clamped plate, there will be a plastic hinge line (a circle). Additional internal work is dissipated on this line.

$$\dot{D}_{hinge} = 2\pi R\frac{2}{\sqrt{3}}M_0\dot{\theta} = 2\pi R\frac{2}{\sqrt{3}}M_0\frac{dw}{dr}\Big|_{r=R} \tag{77}$$

This new term should be added to the right hand side of the rate of work balance expressed by Eq.(65). Assuming the same velocity field as in the case of the simply supported plate, the contribution of the new term can be easily evaluated and the expression for the collapse load becomes,

$$p^* = \frac{M_0}{R^2}\frac{4}{\sqrt{3}}(1 + \frac{2}{n})\left[\sqrt{n^2 - n + 1} + n\right] \tag{78}$$

14

The plot of the dimensionless collapse pressure versus the parameter n is shown on page 12. The minimum is seen to occur at $n = 0.91$. The corresponding value of the upper bound on the collapse load is $p^* = 13.8$ which is almost twice a similar value for the simply supported plate.

It is interesting to compare the velocity profile for both types of boundary conditions, see below. In both cases the velocity field is close to a conical shape but there is a qualitative difference. The curvature of the simply supported plate is positive forming a dish with a slope at the center. The curvature in the clamped plate is negative so that a cusp is formed with a discontinuous slope at the center. This difference could be clearly seen from a blown-up graph of the velocity field near the center of the plate.

4.3 Plastic Resistance of a Circular Membrane

Let us consider a similar problem of a thin circular membrane under a uniformly distributed pressure, discussed in Section 4.2.3 of Part I. The only difference is that the membrane is rigid-plastic. From the strain-displacement relation, Eq.(206 of Part I) we can calculate the rate of strains

$$\dot{\varepsilon}_{rr} = \frac{\delta \dot{u}_r}{\delta r} + \frac{\delta w}{\delta r} \frac{\delta \dot{w}}{\delta r} \tag{79}$$

$$\dot{\varepsilon}_{\theta\theta} = \frac{\dot{u}_r}{r} \tag{80}$$

Assuming that $\dot{u}_r = 0$ meaning that trajectories of all material points move vertically, Eqs.(79) and (80) reduce to

$$\dot{\varepsilon}_{rr} = \frac{\delta w}{\delta r} \frac{\delta \dot{w}}{\delta r}, \quad \dot{\varepsilon}_{\theta\theta} = 0 \tag{81}$$

From the above information one can uniquely determine the components of the membrane forces. Because the radial and circumferential directions are principal directions, Eq.(44) in expanded notation gives

$$N_r = \sqrt{\frac{1}{3}} N_0 \frac{2\dot{\varepsilon}_{rr} + \dot{\varepsilon}_{\theta\theta}}{\sqrt{(\dot{\varepsilon}_{rr}^2 + \dot{\varepsilon}_{vv}\dot{\varepsilon}_{\theta\theta} + \dot{\varepsilon}_{\theta\theta}^2)}} \tag{82}$$

$$N_\theta = \sqrt{\frac{1}{3}} N_0 \frac{2\dot{\varepsilon}_{\theta\theta} + \dot{\varepsilon}_{rr}}{\sqrt{(\dot{\varepsilon}_{rr}^2 + \dot{\varepsilon}_{vv}\dot{\varepsilon}_{\theta\theta} + \dot{\varepsilon}_{\theta\theta})}} \tag{83}$$

Substituting the expression for the strain rates given by Eq.(81) to Eq.(83), the corresponding membrane forces are

$$N_{rr} = \frac{2}{\sqrt{3}} N_0, \quad N_{\theta\theta} = \frac{1}{\sqrt{3}} N_0 \tag{84}$$

Such a field of membrane forces is approximate, as it does not satisfy the symmetry condition $N_r = N_\theta$ at the plate center. This is a consequence of a simplified assumption $\dot{u}_r = 0$.

The surface element in the membrane is subject to bi-axial tension of a constant magnitude over the structure no matter what is the size and shape of the function $w(r)$. This is a great simplification because the terms N_{rr} is a constant in the equation of equilibrium (205 in Part I),
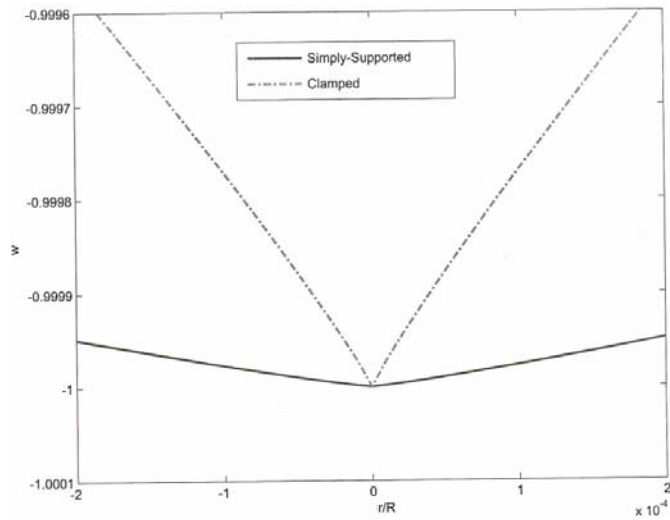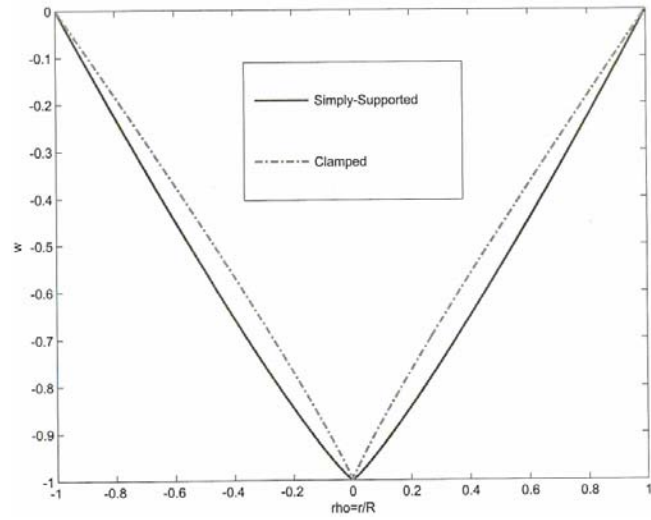
$$N_0 \frac{2}{\sqrt{3}} \frac{d}{dr}(r \frac{dw}{dr}) + rp = 0 \tag{85}$$

Integrating the above equation twice one gets

$$w(r) = -\frac{\sqrt{3}}{8} \frac{pr^2}{N_0} + C_1 \ln r + C_2 \tag{86}$$

The integration constant C_1 should vanish because otherwise the central deflection of the membrane will go to infinity. The integration constant C_2 is found from zero displacement at the clamped edge $w(r = R) = 0$. The final solution is
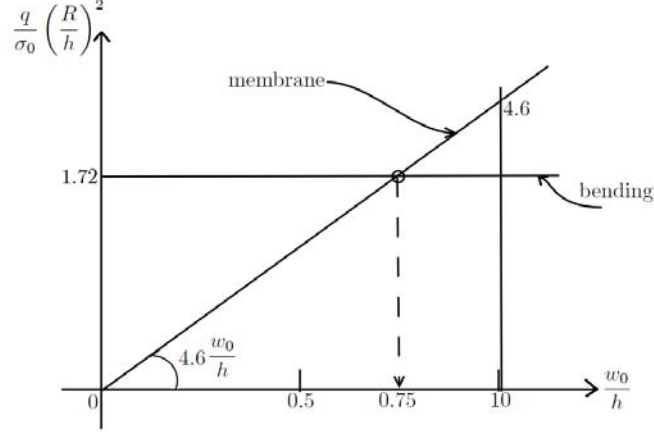
$$w(r) = \frac{\sqrt{3}pR^2}{8N_0}(1 - (\frac{r}{R})^2) \tag{87}$$

15

In particular, the relation between the pressure and the central deflection w_0 is

$$p = \frac{8}{\sqrt{3}}\sigma_0\left(\frac{h}{R}\right)^2\frac{w_0}{h} \tag{88}$$

A comparison of the bending and membrane solutions is presented in the figure.

A transition between the bending and membrane response (intersection point of two lines), occurs when central deflection reaches $\frac{3}{4}$ of the thickness. In reality a transition from bending to membrane action occurs more gradually when deflection becomes of an order of plate thickness. Despite the approximate nature of the above analytical solution with zero in-plane displacement and parabolic shape of the transverse deflection $w(r)$, its accuracy is very good. This can be seen from a comparison of the prediction of Eq.(87) with the finite element calculation, shown in the figure below.
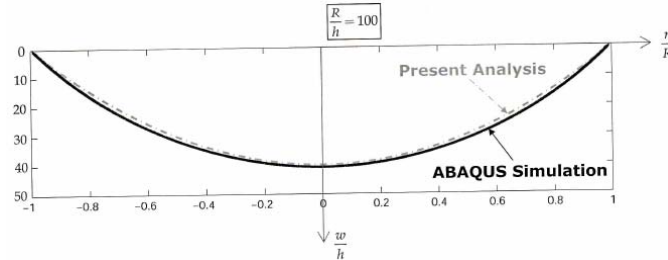
4.4   Axial Crushing of a Prismatic Tube

The prismatic tube of a circular cross-section subjected to large axial load deforms plastically in the axi-symmetric or diamond mode. Thicker tubes with the radius-to-thickness ratio $R/h < 20$ fold by forming axi-symmetric bellows while thinner tubes crumple in the diamond mode, as shown in the figure below. When the loading and respons is rotationally symmetric, the in-plane shear forces and twisting moment vanish, $N_{r\theta} = M_{r\theta} = 0$ and the components of the generalized forces become

$$N_{\alpha\beta} = \begin{vmatrix} N_\theta & 0 \\ 0 & N_z \end{vmatrix}, \quad M_{\alpha\beta} = \begin{vmatrix} M_\theta & 0 \\ 0 & M_z \end{vmatrix} \tag{89}$$

In the absence of a lateral pressure, the principle of virtual velocities, Eq.(51) reduces to

$$\int_S (M_{\alpha\beta}\dot{\kappa}_{\alpha\beta} + N_{\alpha\beta}\dot{\varepsilon}_{\alpha\beta})ds = \int_\Gamma \bar{N}_z\dot{u}_z d\Gamma = P\dot{u} \tag{90}$$

where $\dot{u}$ is a uniform compressive rate of displacement and $P = 2\pi R\bar{N}$ is the total (still unknown) compressive force. Further simplifications are introduced by making assumptions about the strain rate field. It was observed

in tests that the tube walls are inextensible in the axial direction so that $\dot{\varepsilon}_z = 0$. Furthermore, the change in the circumferential curvature is much smaller than in the axial curvature, thus $\dot{\kappa}_\theta = 0$. The integrand of Eq.(90) reduces to $(M_z\dot{\kappa}_z + N_\theta\dot{\varepsilon}_\theta)$, where (M_z, M_θ) are related by the yield condition.

Finally, the square yield condition, circumscribed on the exact yield condition (see p. 8 of Part II) is assumed and the stress state is approximated by $M_z = M_0$ and $N_\theta = N_0$. Now, the principle of virtual velocities is reduced to

$$2\pi R[M_0 \int_L \dot{\kappa}_z dz + N_0 \int_L \dot{\varepsilon}_\theta dz] = P\dot{u} \tag{91}$$

The bending and membrane rate of energies are calculated separately by assuming a suitable deformation mode. The first observation is that the process of plastic folding is progressive with one fold formed at a time. Therefore, the integration over the lateral surface can be performed over the length 2H of the folding wave.
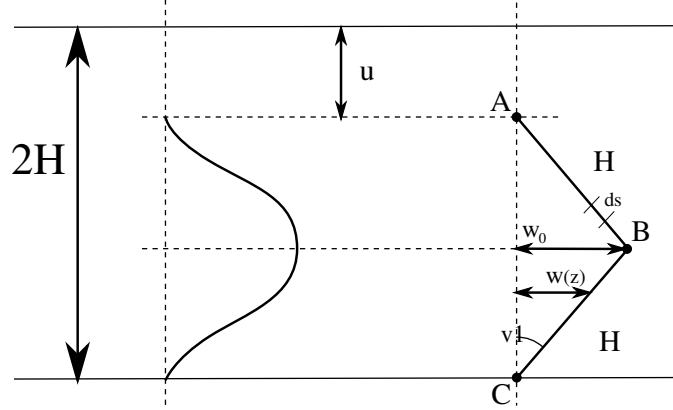
In an actual metal tube the folds are smooth and continuous. The computational model is simplified and consists of straight segments between the hinge circles. Taking the angle α as the process parameter, the tube shortening is $u = 2H(1 - \cos\alpha)$, and its rate is $\dot{u} = 2H\dot{\alpha}\sin\alpha$. The instantaneous amplitude of the lateral velocity is $\dot{w} = H\dot{\alpha}\cos\alpha$.

The bending rate of energy is calculated first:

$$\dot{E}_b = 2\pi R M_0 \int_{2H} \dot{\kappa}_z dz = 2\pi R M_0 \sum_{i=1}^{3} |\dot{\theta}_i| \tag{92}$$

There are three plastic hinge circles A, B, C where the rate of rotation are $\dot{\theta}_A = \dot{\alpha}$, $\dot{\theta}_B = 2\dot{\alpha}$, and $\dot{\theta}_C = \dot{\alpha}$. Thus, Eq.(92) yields $\dot{E}_b = 8\pi R M_0 \dot{\alpha}$. The hoop strain rate is defined by

$$\dot{\varepsilon}_\theta = \frac{\dot{w}}{R} \tag{93}$$

and thus the rate of membrane energy is

$$\dot{E}_m = 2\pi R N_0 \cdot 2 \int_0^H \frac{\dot{w}_0}{R} ds \tag{94}$$

where ds is the element length of the fold and the coefficient 2 accounts for the two halves. In the present model the instantaneous velocity field is a linear function of the deformed coordinates

$$\dot{w}(s) = \dot{w}_0 \frac{s}{H} \tag{95}$$

Performing the integration, the final expression for the rate of membrane energy is

$$\dot{E}_m = 2\pi N_0 \dot{w}_0 H^2 \tag{96}$$

Substituting the calculated values into the principle of virtual velocity, Eq.(91) gives

$$2HP\dot{\alpha}\sin\alpha = 8\pi M_0\dot{\alpha} + 2\pi N_0\dot{\alpha}\frac{H^2}{R}\cos\alpha \tag{97}$$

where α changes from $\alpha = 0$ at the beginning of the process to $\alpha = \frac{\pi}{2}$ at the end. Integrating Eq.(97) with respect to the process parameter α gives an expression for the mean crushing force P_m:

$$P_m = \frac{2\pi^2 M_0}{H} R + \pi N_0 H \tag{98}$$

The dependence of the mean crushing force on the unknown length H of the folding wave is shown in the figure below.
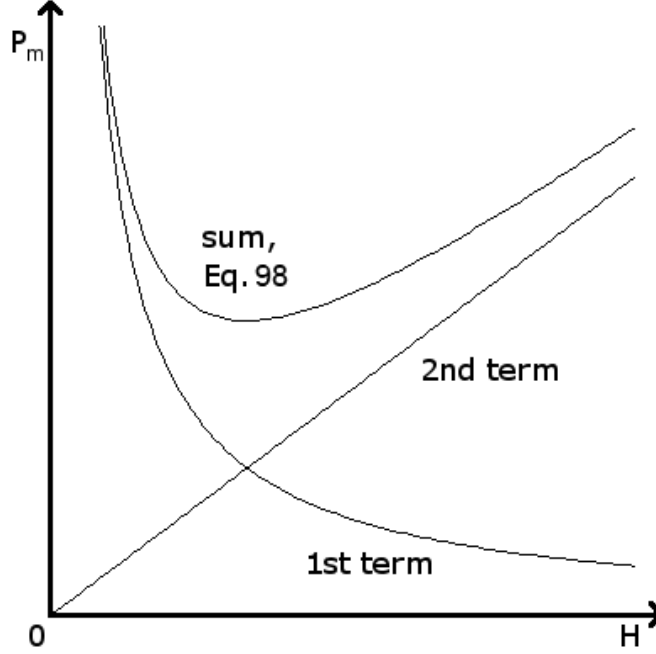
It is plausible to assume that the folding wave adjusts itself in the crushing process to minimize the magnitude of the mean crushing force. Indeed, the analytical minimum exists when

$$\frac{dP_m}{dH} = -\frac{2\pi^2 M_0}{H^2} R + \pi N_0 = 0 \tag{99}$$

from which the optimum value of H is found

$$H_{opt} = \sqrt{\frac{2\pi M_0 R}{N_0}} \tag{100}$$

Substituting Eq.(100) back into Eq.(98), the best estimate of the mean crushing force is

$$P_m = 2\pi \sqrt{2\pi M_0 N_0 R} \tag{101}$$

In the literature, analytical expressions for the normalized mean crushing force were derived. Dividing both sides of Eq.(101) by M_0, the dimensionless mean crushing force becomes a function of the diameter-to-thickness ratio:

$$\frac{P_m}{M_0} = 2\pi\sqrt{4\pi}\sqrt{\frac{2R}{h}} \approx 22.27\sqrt{\frac{2R}{h}} \tag{102}$$

In physical quantities using the definitions of M_0 and N_0, Eq.(102) reads

$$P_m = 7.87\sigma_0 h^{\frac{3}{2}} R^{\frac{1}{2}} \tag{103}$$

In reality, not the entire crushing distance $2H$ is available. The tube shortening during the formation of a typical fold is $0.75(2H)$. With the correction for the effective crushing distance, the coefficient in Eq.(103) is increased, to give

$$P_m = 9.44\sigma_0 h^{\frac{3}{2}} R^{\frac{1}{2}} \tag{104}$$

19

Despite many simplifying assumptions, the present solution provides a good estimate of the mean crushing force and energy absorption of tubes. The prediction of Eq.(104) is compared with test results and other solutions in the graph below.
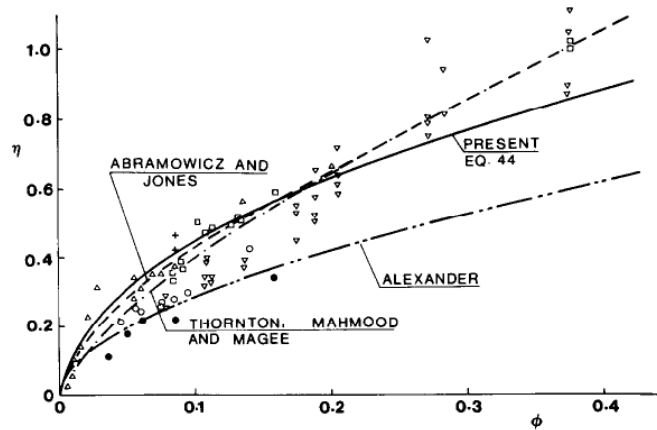
Courtesy Elsevier, Inc., `http://www.sciencedirect.com`. Used with permission.

The dimensional coordinates in the above figure are defined by the quantities:

$$\eta = \frac{P_m}{2\pi R_0 h_0 \sigma_0}$$

$$\phi = \frac{2h}{R}$$

For a more detailed exposition of the theory and examples, the following two references are suggested.

Sawczuk, A. Mechanics and Plasticity of Structures. New York, NY: Halsted Press, 1989.

Hodge, Philip G. Plastic Analysis of Structures. New York, NY: McGraw-Hill, 1959.